Journal of Materials Processing Tech. 247 (2017) 243–256

Contents lists available at ScienceDirect

Journal of Materials Processing Tech.

journal homepage: www.elsevier.com/locate/jmatprotec

Investigation of post-weld rolling methods to reduce residual stress and distortion

Luis D. Cozzolino[a,*], Harry E. Coules[b], Paul A. Colegrove[a], Shuwen Wen[c]

[a] Cranfield University, Cranfield, Bedfordshire MK43 0AL, UK
[b] Department of Mechanical Engineering, University of Bristol, Bristol BS8 1TR, UK
[c] Tata Steel R, D & T, Swinden Technology Centre, Rotherham, South Yorkshire S60 3AR, UK

ARTICLE INFO

Keywords:
Residual stress management
Rolling
Welding
Modelling
FEA

ABSTRACT

The mechanisms of post-weld rolling and how it reduces and eliminates residual stress and distortion are poorly understood. Finite element analysis was applied to two different methods of rolling: rolling the weld bead directly with a single roller and rolling beside the weld bead with a dual flat roller. The models showed that both rolling techniques were able to induce compressive stress into the weld region, which increased with rolling load. The distribution of stress was sensitive to the coefficients of friction between the workpiece and the roller and the backing bar. High friction coefficients concentrated the plastic deformation and compressive stress within the centre of the weld bead. Distortion can be eliminated by rolling; however, the experiments indicated that this was only achieved when applied to the weld bead directly.

1. Introduction

Fusion welding involves uneven heating of the weldments, which causes a non-uniform temperature distribution and consequently local plastic strain in the weld and surrounding metal, as described in (Connor, 1987). The mismatch of the plastic strains between the weld and the parent metal causes residual stresses, which can have adverse effects on the mechanical properties and usually result in distortion.

To understand the generation of residual stress, computational weld mechanics can be used to simulate the large-scale effect of the heat source, as described by Lindgren (2007). Many simplifications may be adopted, which allow accurate results to be obtained in a relatively short time. Additionally, welding simulation can significantly reduce the number of experiments required to test particular design conditions to a few key ones for validating the models.

There are a number of residual stress mitigation techniques that can be used. Rolling is one that is effective, but has received relatively little attention in the literature. Kurkin and Tsyao (1962) analysed its beneficial effect in titanium alloys (OT4-1, VT-1, VT5-1), while Kurkin and Anufriev (1984) in aluminium alloys (Amg6 and 1201), obtaining significant residual stress reduction. Altenkirch et al. (2009) demonstrated its effectiveness for aluminium friction stir welds (FSW). In addition, numerical simulations conducted by Wen et al. (2010) in FSW, and Yang and Dong (2011) in low carbon steel TIG welds, have obtained results in agreement with the experimental findings. Recently, experiments conducted by Coules et al. (2013a, 2013b, 2012b) demonstrated how post-weld rolling can reduce distortion, and residual stress in Gas Metal Arc Welds (GMAW) in S355JR steel plates.

The process works by inducing positive local plastic strain in the welding direction, which counteracts the negative plastic strain generated during welding, as shown experimentally by Altenkirch et al. (2009), and the numerical models of Wen et al. (2010) for FSW, as well as by Yang et al. (1998) in TIG welds of aluminium alloy. Post-weld rolling is normally applied on top of the weld, by means of a single roller and is shown in Fig. 1(a). However, the technique can be applied with two rollers beside the weld bead which has been used to reduce the incidence of solidification cracking (Fig. 1(b)), as shown by Liu et al. (1996) in fusion welds of 2024-T4 aluminium alloy. Furthermore, fatigue cracks usually start from the weld toes, as shown by Tryfyakov et al. (1993). In this study deformation of the weld toes by ultrasonic impact peening treatment reduced the stress concentration caused by this region. In addition, McClung (2007) showed that tensile residual stress reduces the fatigue life of weldments. Therefore, post-weld rolling of the weld toes could potentially reduce these problems by reshaping the weld bead and inducing a compressive residual stress in the weld bead and surrounding metal.

In this paper, we describe the use of numerical models to predict the effect of post-weld rolling both on top of the weld bead using a grooved roller, and rolling beside the weld bead with a dual flat roller. The effects of parameters such as rolling load, roller position and width and

* Corresponding author.
E-mail address: daniel.cozzolino@outlook.com (L.D. Cozzolino).

http://dx.doi.org/10.1016/j.jmatprotec.2017.04.018
Received 26 August 2016; Received in revised form 20 April 2017; Accepted 23 April 2017
Available online 27 April 2017

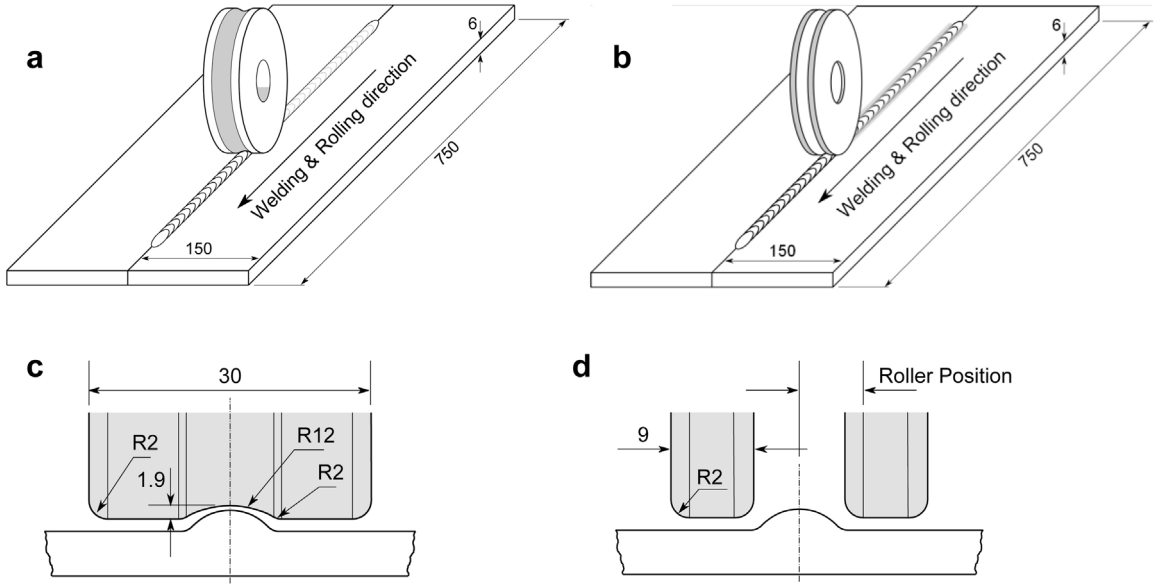

Fig. 1. Geometry and rolling methods for (a) rolling on top of the weld bead and (b) rolling beside the weld bead with the dual flat rollers; (c) roller dimensions used for rolling on top of the weld bead and (d) parameterised roller dimensions for rolling beside the weld bead (dimensions in mm).

their influence on the welding residual stress and distortion are determined and compared with equivalent experiments by Coules et al. (2013b). In addition, the influence of friction between the backing-bar, workpiece, and roller were also investigated.

2. Methodology

2.1. Numerical models

Linear single-pass bead-on-plate Gas Metal Arc Welds in rectangular plates of S355JR structural steel, and the subsequent rolling of these welds, were simulated using the finite element method. The models were run with Abaqus Standard version 6.9 as a sequentially coupled thermal-mechanical analysis. They consist of two main steps, namely a welding thermal-mechanical step to predict the welding-induced residual stress, and a rolling step to alter the residual stress formed from welding. A single set of welding parameters which are described in Section 2.2 were used for all the models.

2.1.1. Thermal model of the welding process

The models were three dimensional and simulate bead-on-plate welds on flat profile plates. Owing to the geometry of the experiments and to reduce computational time, only half of the geometry was modelled, which was also used for the subsequent rolling mechanical models. A typical mesh is shown in Fig. 2(a). A denser mesh was implemented on the weld bead region and on areas where rolling was subsequently applied. The effect of the mesh density was studied to ensure that the results presented are independent of the mesh size. The dimensions of half of the workpiece were 750 × 150 × 6 mm, and the weld seam was 600 mm in length. The average weld bead dimensions, measured by Coules et al. (2013a, 2013b, 2012b, 2012c) were Ø = 13.8, H = 2.9 and W = 5.6 mm.

The weld bead in these models was active during the entire welding step as well as the subsequent ones; hence the "dumped block" method, explained by Shan et al. (2007) was used and has sufficient accuracy for this work. Convective and thermal radiation heat losses were included from the top surface of the workpiece using a convective coefficient of 10 W m^{-2} $°C^{-1}$, as recommended by M. C. Smith and A. C. Smith (2009) for stainless steel bead-on-plate welds, and an emissivity of 0.8 was used as suggested by Simonson (1967). Even though the backing support was composed of both copper (underneath the weld bead) and aluminium in the far field, it was modelled with a temperature dependent convective heat transfer coefficient given by:

$$h(T) = ae^{bT} + c \tag{1}$$

where h is the convective heat transfer coefficient, and $a = 505.65$, $b = 158.89 \times 10^{-5}$, and $c = -400$ are constants which were determined by trial and error. The welding heat, q was applied in all the models with a double ellipsoid volumetric heat source distribution proposed by Goldak et al. (1984):

$$q = \frac{6\sqrt{3} f_f Q}{a_f bc\pi\sqrt{\pi}} e^{-3x^2/a_f^2} e^{-3y^2/b^2} e^{-3z^2/c^2} \quad ifx \geq 0$$
$$q = \frac{6\sqrt{3} f_r Q}{a_r bc\pi\sqrt{\pi}} e^{-3x^2/a_r^2} e^{-3y^2/b^2} e^{-3z^2/c^2} \quad ifx < 0 \tag{2}$$

where a_f, a_r, b, and c are geometrical factors for the ellipsoidal shape; x, y, and z are the coordinates of the geometry, f_f and f_r are the heat input fraction in the front and rear ellipsoid quadrants, and their summation must equal two. Finally, Q is the welding power.

Since the weld bead was entirely present during the welding step, the double ellipsoid heat input was centred on the top of it, as shown in Fig. 3. Owing to the mismatch between the weld bead and double ellipsoid shapes, not all the heat in the double ellipsoid was actually applied to the weldment. The geometrical parameter of the double ellipsoid were considered initially as 90% of the molten region observed in the experiment, as proposed by Goldak and Akhlaghi (2005); however this approach did not produce a good match with the temperature profiles obtained in the experiments. Therefore, these parameters (af, ar, b, c) were tuned manually until a good match with the temperature profile was obtained. The final values were smaller than 90% of the weldpool dimensions.

In Table 1 the parameters for the Goldak double ellipsoid heat source are reported.

Temperature dependent thermal properties used are reported in Fig. 4 (Thompson et al., 2008). Michaleris and Debiccari (1997) sugested to artificially increase the thermal conductivity above the melting point to take into account the stirring effect present in the weld pool. The latent heat of fusion, 272 kJ kg^{-1} K (Al-Sulaiman et al., 2007), and of vaporisation, 6258 kJ kg^{-1} K (Al-Sulaiman et al., 2007), were included in the analysis between 1500 and 1530 °C, and 3090 and 3100, respectively.

After the heat induced by the welding process was finished, an additional 600 s cooling step was applied to allow the weldment to cool